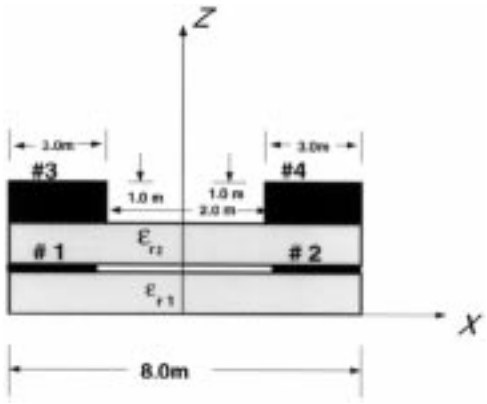

Fig. 4. Two conducting strips (3.0-m width) and two conducting cylinders of rectangular cross section (3.0 m × 1.0 m) mounted over two dielectric beds. The whole structure is situated on a ground plane. The length of the structure in y-dimension is 10 m.

TABLE II
CAPACITANCE MATRIX FOR THE FOUR-CONDUCTOR SYSTEM (CAPACITANCE IN NANO-FARADS)

$\epsilon_{r1}=1.0, \epsilon_{r2}=1.0$				$\epsilon_{r1}=60.0, \epsilon_{r2}=30.0$			
0.67	-0.01	-0.29	-0.01	27.33	-0.27	-8.13	-0.16
-0.01	0.67	-0.01	-0.29	-0.27	27.33	-0.16	-8.13
-0.29	-0.01	0.64	-0.09	-8.50	-0.13	9.23	-1.46
-0.01	-0.29	-0.09	0.64	-0.13	-8.50	-1.46	9.23

strips are modeled with 60 triangular patches each. The conducting cylinders and dielectric beds are modeled in the same way as in the previous example. The total number of unknowns for this case is 1248. In Table II, we present the capacitance matrix for two dielectric ratios, which again, remains symmetric.

V. CONCLUSIONS

In this paper, we present a superior method to calculate the charge distribution and capacitance for a system of finite-sized conductors in the presence of arbitrarily shaped dielectric bodies of low, as well as high, dielectric materials.

REFERENCES

[1] S. M. Rao, T. K. Sarkar, and R. F. Harrington, "The electrostatic field of conducting bodies in multiple dielectric media," *IEEE Trans. Microwave Theory Tech.*, vol. MTT-32, pp. 1441–1448, Nov. 1984.
[2] K. Nabors and J. White, "Fastcap: A multipole accelerated 3-D capacitance extraction," *IEEE Trans. Computer-Aided Design*, vol. 11, pp. 1447–1459, Oct. 1991.
[3] X. Cai, K. Nabors, and J. White, "Efficient Galerkin techniques for multipole-accelerated capacitance extraction of 3-D structures with multiple dielectrics," presented at the Proc. Conf. Advanced Res. VLSI, Chapel Hill, NC, 1995.
[4] R. F. Harrington, *Field Computation by Moment Methods.* New York: Macmillan, 1968.
[5] S. V. Yeshantharao, "EMPACK—A software toolbox of potential integrals for computational electromagnetics," M.S. thesis, Dept. Elect. Eng., Univ. Houston, Houston, TX, 1989.

Analysis of a Slot-Coupled T-Junction Between Circular-to-Rectangular Waveguide

S. B. Sharma, S. B. Chakrabarty, and B. N. Das

***Abstract*— This paper presents a rigorous analysis of a slot-coupled T-junction between a primary circular cylindrical waveguide and rectangular waveguide, forming the coupled T-arm. The analysis is based on moment-method formulation using full-wave basis functions and Galerkin's technique for testing. Expression for the coupling and reflection coefficients are found, taking into account the effect of finite wall thickness of the circular waveguide in which the coupling slot is milled. A comparison between the theoretical and experimental results on coupling and return loss are presented.**

I. INTRODUCTION

In view of their wide application in commercial systems as well as laboratory measurements [1]–[5], investigation into different types of aperture-coupled waveguide junctions has attracted the attention of researchers for a long time. Rigorous analysis on the slot-coupled junction between similar and dissimilar waveguides with collinear [6], [7] and orthogonal axes [8] have been carried out. Formulation has been presented for a T-junction [9] and also cascaded sections of junctions [10], in which the primary guide is a rectangular waveguide and the T-arm is a circular waveguide. It is also of importance to study the electrical characteristics of a T-junction, in which the primary waveguide is a circular cylindrical waveguide and the secondary guide is a rectangular waveguide. This was presumably not attempted because of the complexity in finding the internal dyadic Green's function of the circular cylindrical waveguide.

In this paper, analysis based on moment-method formulation using full-wave basis function and the Galerkin's method for testing is presented for derivation of expression for the electrical characteristics of a T-junction between a circular waveguide as the primary waveguide and T-arm as the rectangular waveguide. The coupling takes place through an axial slot in the wall of circular waveguide and in the transverse cross section of the coupled rectangular waveguide. This analysis takes into account the effect of finite wall thickness by considering the possible forward and backward traveling waves in the stub waveguide representing the coupling slot milled in the wall of the cylindrical waveguide of finite wall thickness [11]. The unknown field distribution in the slot aperture is found by transforming the integral equation derived from the boundary conditions for the tangential components of the magnetic fields into a matrix equation. The elements of the matrices are found considering the effect of all possible higher order modes in circular, rectangular, and stub waveguides. From the elements of the scattering matrix derived in this formulation, coupling and return loss are found. A comparison between the theoretical and experimental results are also presented.

Manuscript received April 24, 1997; revised May 11, 1998.

S. B. Sharma and S. B. Chakrabarty are with the MSAD/MSDG/RSA Group, Space Applications Centre, Indian Space Research Organization, Ahmedabad 380 053, India.

B. N. Das is with the Department of Electronics and Electrical Communication Engineering, Indian Institute of Technology, Kharagpur 721 302, India.

Publisher Item Identifier S 0018-9480(98)05499-4.

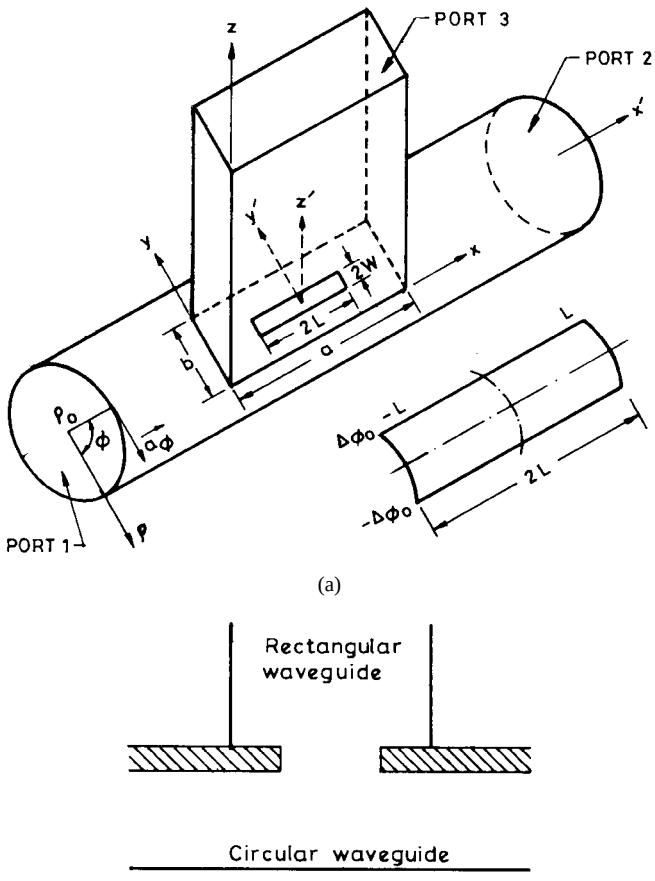

Fig. 1. A T-junction between circular and rectangular waveguides.

II. General Analysis

Fig. 1 shows the geometry of a T-junction between a circular cylindrical waveguide and rectangular waveguide coupled through an axial slot of length $2L$ and width $2W(=2a\Delta\Phi_0)$ in the wall of a circular cylindrical waveguide. The coupling slot is in the form of a curvilinear rectangle on the wall of the circular waveguide. Since, the angular width $2\Delta\Phi_0$ is small, the curvilinear rectangle can be replaced by a planar rectangle for the purpose of analysis.

For finite wall thickness "t" of the wall of the circular waveguide, the coupling slot can be considered as a short section of a rectangular waveguide (designated as the stub waveguide), the expanded view of which is shown in Fig. 2. For $2a\Delta\Phi_0$ small compared to L, the electric-field intensity along the width of the coupling slot can be assumed to be constant and the analysis is carried out from the continuity of tangential magnetic fields at the interfaces I–IV of Fig. 2 for all possible excitations.

In Fig. 1, the expression for the coupling between ports 1 and 3 and the reflection coefficient seen from port 1 are derived for the signal fed to port 1.

Following the procedure used in [9], the expression for the field at the interface C is

$$[E^C] = \{[U] + [B][Y^{\rm rw}]^{-1}[h^{\rm rw}][B]\}[E^+]_{III} \tag{1}$$

where

$$[E^+]_{III} = \{[Y^{\rm cw}]^{-1}[h^{\rm cw}[B][Y^{\rm rw}]^{-1}[h^{\rm rw}[B] - [U]\}^{-1} \times [Y^{\rm cw}]^{-1}[h^{\rm inc}]. \tag{2}$$

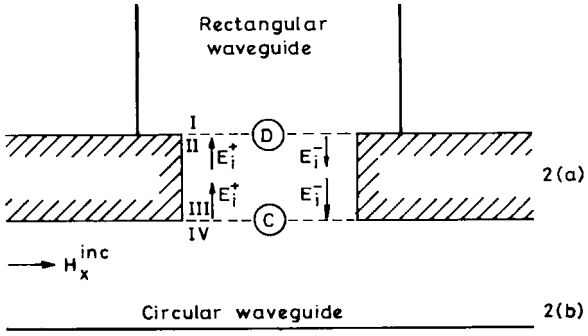

Fig. 2. An expanded view of the slot as stub waveguide.

The elements of the column matrix $[h^{\rm inc}]$ are given by

$$h_s^{\rm inc} = \langle H_{x'}^{\rm inc}, w_s\rangle. \tag{3}$$

$H_x^{\rm inc}$ is given by [12]

$$H_x^{\rm inc} = \frac{k_c^2}{j\omega\mu}\sqrt{\frac{2}{\pi[(x'_{11})^2-1]}}\cos\phi e^{-j\beta_{11}x} \tag{4}$$

where x'_{11} is the first root of $J'_1(x)=0$, the derivative of the first-order Bessel function. $\beta_{11} = k\sqrt{1-(x'_{11}/\rho_0 k)^2}$, $k(=2\pi/\lambda)$ being the wavenumber in free space.

In a similar fashion, the total tangential electric field in the aperture plane of the slot at the interface D is given by

$$[E^D] = \{[B] + [Y^{\rm rw}]^{-1}[h^{\rm rw}][B]\}[E^+]_{III}. \tag{5}$$

In (1), (2), and (5), $[B]$ is the diagonal matrix with diagonal elements $\exp(-j\gamma_{i0}t)$, t is the thickness of the waveguide, γ_{i0} is the propagation constant of the ith mode in waveguide section (C)–(D), $[U]$ is the unit matrix, and $[Y^{\rm rw}]$, $[h^{\rm rw}]$ and $[Y^{\rm cw}]$, $[h^{\rm cw}]$ are square matrices whose elements are given by

$$Y_{ps}^{\rm rw} = \langle \xi^r(e_p), w_s\rangle + Y_p 2LW\delta_{ps} \tag{6}$$

$$h_{is}^{\rm rw} = -\langle \xi^r(e_i), w_s\rangle + Y_i 2LW\delta_{is} \tag{7}$$

$$Y_{ps}^{\rm cw} = \langle \xi^r(e_p), w_s\rangle - Y_p 2LW\delta_{ps} \tag{8}$$

$$h_{is}^{\rm cw} = -\langle \xi^r(e_i), w_s\rangle - Y_i 2LW\delta_{is}. \tag{9}$$

δ is the Kronecker delta and the symbol $\langle\,\rangle$ represents the inner product. $\xi^r(e_j)(j = i \text{ or } p)$ (6)–(9) is related to the transverse component of the magnetic field in the stub waveguide by the relation [9]

$$H_x^r = E_j\xi^r(e_j), \qquad j = p, i. \tag{10}$$

The functions e_p and e_i are the dimensionless quantities given by

$$e_j(x') = \sin\frac{j\pi}{2L}(x'+L), \qquad j = p, i \tag{11}$$

and

$$w_s = \sin\frac{s\pi}{2L}(x'+L). \tag{12}$$

III. Expressions for the Elements of the Matrices

Using (3), (4), and (12), and carrying out the integration over the slot aperture, the elements of the column matrix $[h^{\rm inc}]$ are obtained as

$$h_s^{\rm inc} = \frac{k_c^2}{j\omega\mu}\sqrt{\frac{2}{\pi(x'^2_{11}-1)}}\,2W \times \frac{\left(\frac{s\pi}{2L}\right)[(-1)^s e^{-j\beta_{11}L} - e^{j\beta_{11}L}]}{\beta_{11}^2 - \left(\frac{s\pi}{2L}\right)^2}. \tag{13}$$

The expression for $Y_{ps}^{\rm rw}$ and $h_{is}^{\rm rw}$ are found following the method suggested in [8].

The derivation of the expression for $Y_{ps}^{\rm cw}$ and $h_{is}^{\rm cw}$ can be found only after the derivation of the expression for $H_x^{\rm cw}(e_p)$ due to an axial slot in the primary circular waveguide.

The magnetic field in the primary waveguide due to aperture field distribution in the plane of the slot is expressed as

$$H_x^{\rm cw} = \iint -\overline{u}_r \times (-\overline{u}_\theta) E_p . \overline{\overline{U}}_r \, ds \tag{14}$$

where $\overline{\overline{U}}_r$ is the dyadic Green's function in the primary waveguide (circular waveguide) and is given by

$$\overline{\overline{U}}_r = \frac{j}{\omega\mu}(k^2\overline{\overline{I}} + \nabla\nabla)\overline{\overline{G}}(\rho,\, \rho_0) \tag{15}$$

where k is the wavenumber and $\overline{\overline{I}}$ is the unit Dyadic, and $\overline{\overline{G}}(\rho,\, \rho_0)$ is given by

$$\overline{\overline{G}}(\rho,\, \rho_0) = \sum_{n=0}^{\infty}\sum_{m=1}^{\infty} \frac{\epsilon_n}{2\pi\rho_0^2\gamma_{mn}} \cos\, n(\phi-\phi') \times \frac{J_n\left(x'_{mn}\,\frac{\rho}{\rho_0}\right)}{J_n(x'_{mn})} \frac{e^{\pm\gamma_{mn}(x-x')}}{1-\frac{n^2}{x'^2_{mn}}} \tag{16}$$

where x'_{mn} is the mth root of the derivative of the nth-order Bessel function.

From (14) to (16), $H_x^{\rm cw}$ at the slot aperture (lower interface) is given by

$$H_x^{\rm cw} = \frac{1}{j\omega\mu}\left(k^2+\frac{\partial^2}{\partial x^2}\right)\sum_{n=0}^{\infty}\sum_{m=1}^{\infty} \times \frac{\epsilon_n}{2\pi\rho_0^2\gamma_{mn}} \frac{1}{1-\frac{n^2}{x'^2_{mn}}} \int_{-\Delta\phi_0}^{\Delta\phi_0} a\,d\phi' \times \left[e^{-\gamma_{mn}x}\int_{-L}^{x} e^{\gamma_{mn}x'} \sum_p E_p^- \sin\frac{p\pi}{2L}(L+x')\,dx' + e^{\gamma_{mn}x}\int_{x}^{L} e^{-\gamma_{mn}x'} \sum_p E_p^- \sin\frac{p\pi}{2L}(L+x')\,dx'\right]. \tag{17}$$

Carrying out the proper mathematical operation, the expression for the magnetic field is obtained as

$$H_x^{\rm cw} = \frac{2W}{j\omega\mu}\sum_{n=0}^{\infty}\sum_{m=1}^{\infty} \frac{\epsilon_n}{2\pi\rho_0^2\gamma_{mn}} \frac{\cos\, n\phi}{1-\frac{n^2}{x'^2_{mn}}} \sum_p E_p^- \frac{\frac{\pi p}{2L}}{\gamma_{mn}^2+\left(\frac{p\pi}{2L}\right)^2} \times \left[(k^2+\gamma_{mn}^2)e^{-\gamma_{mn}L}(e^{-\gamma_{mn}x}-(-1)^p e^{\gamma_{mn}x}) + \left(k^2-\left(\frac{p\pi}{2L}\right)^2\right)2\gamma_{mn}\sin\frac{p\pi}{2L}(L+x)\right]. \tag{18}$$

Using (8), (10), and (17), and carrying out the integration, it is found that

$$Y_{ps}^{\rm cw} = \frac{(2W)^2}{j\omega\mu}\sum_{n=0}^{\infty}\sum_{m=1}^{\infty} \frac{\epsilon_n}{2\pi\rho_0^2\gamma_{mn}} \frac{1}{1-\frac{n^2}{x'^2_{mn}}} \frac{\frac{p\pi}{2L}}{\gamma_{mn}^2+\left(\frac{p\pi}{2L}\right)^2} \times \frac{\frac{s\pi}{2L}}{\gamma_{mn}^2+\left(\frac{s\pi}{2L}\right)^2} 2(k^2+\gamma_{mn}^2) \times \begin{cases} 1+e^{-2\gamma_{mn}L}, & \text{for } p,\ s \text{ odd} \\ 1-e^{-2\gamma_{mn}L}, & \text{for } p,\ s \text{ even} \\ 0, & \text{for } p \text{ odd},\ s \text{ even and } p \text{ even},\ s \text{ odd} \end{cases} + \frac{k^2-\left(\frac{p\pi}{2L}\right)^2}{\gamma_{mn}^2+\left(\frac{p\pi}{2L}\right)^2} 2L\gamma_{mn}\delta_{ps} + Y_p 2LW\delta_{ps} \tag{19}$$

where

$$\epsilon_n = \begin{cases} 2, & \text{for } n=0 \\ 1, & \text{for } n>0 \end{cases}$$

and δ is the Kronecker delta.

IV. Reflection Coefficient at Port 1

The reflection coefficient Γ and the transmission coefficient T are defined as

$$\Gamma = \frac{H^{\rm b.s.}}{H_x^{\rm inc}} \tag{20}$$

$$T = \frac{H_x^{\rm inc}+H_x^{\rm f.s.}}{H_x^{\rm inc}} \tag{21}$$

where $H_x^{\rm b.s.}$ and $H_x^{\rm f.s.}$ are, respectively, the amplitudes of the backward-traveling and forward-traveling waves resulting from the scattering due to the slot.

When the limits of integration x, appearing in (17), is taken to be equal to L, the first term in the square bracket represents the backward-scattered wave $H_x^{\rm b.s.}$ and the second term represents the forward-traveling wave $H_x^{\rm f.s.}$. On carrying out the integrations, the expressions for Γ and T are obtained as a summation of the following form (taking only the dominant mode scattering):

$$\Gamma = \sum_{p=1}^{N} E_p \frac{(k^2-\beta_{11}^2)pW}{jk_c^2\rho_0^2\beta_{11}L}\sqrt{\frac{\pi(x'^2_{11}-1)}{2}} \times \frac{1}{1-\frac{1}{x'^2_{11}}} \frac{e^{j\beta_{11}L}-(-1)^p e^{-j\beta_{11}L}}{\left(\frac{p\pi}{2L}\right)^2-\beta_{11}^2} \tag{22}$$

$$T = 1+\sum_{p=1}^{N} E_p \frac{(k^2-\beta_{11}^2)pW}{jk_c^2\rho_0^2\beta_{11}L}\sqrt{\frac{\pi(x'^2_{11}-1)}{2}} \times \frac{1}{1-\frac{1}{x'^2_{11}}} \frac{e^{j\beta_{11}L}-(-1)^p e^{-j\beta_{11}L}}{\left(\frac{p\pi}{2L}\right)^2-\beta_{11}^2}. \tag{23}$$

V. Coupling Coefficient Between Ports 1 and 3

The expression for the coupling coefficient in this case is the same as that in [8], multiplied by the following term:

$$r = \sqrt{\frac{y_{\rm rw}}{y_{\rm cw}}} \tag{24}$$

where $y_{\rm cw}$ and $y_{\rm rw}$ are the dominant mode characteristic admittances of rectangular and circular waveguides, respectively.

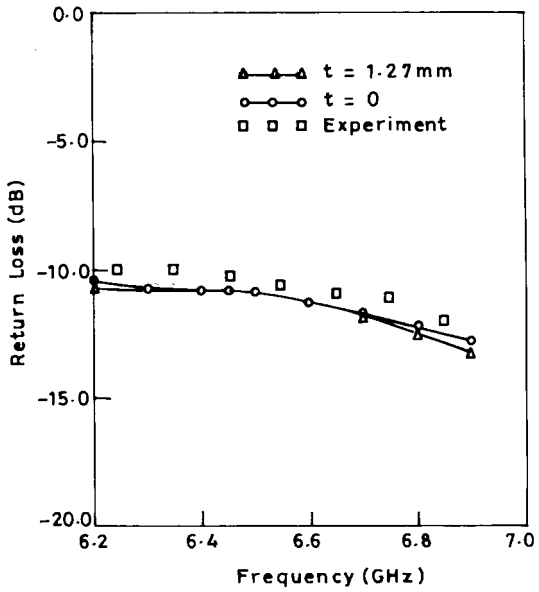

Fig. 3. Variation of return loss seen from port 1 of Fig. 1.

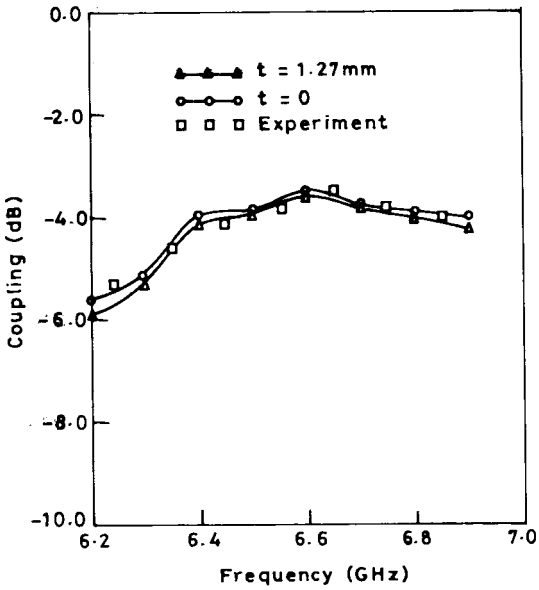

Fig. 4. Variation of coupling from port 1 to 3 of Fig. 1.

VI. Numerical Results and Discussion

Using (1)–(12) and (22), the variation of the return loss at port 1 is evaluated for $2L = 23.31$ mm and $2W = 2$ mm over the frequency range from 6.2 to 6.9 GHz. The theoretical result on return loss seen from port 1 is evaluated for $t = 0$ mm as well as $t = 1.27$ mm. The data are presented in Fig. 3, together with the experimental data recorded with an HP8510C network analyzer. The waveguide dimension for the circular waveguide is 32.54 mm and the length of the circular waveguide is 104 mm. WR137 is used for the rectangular waveguide. The theoretical result on coupling from ports 1 to 3, as well as the experimental data, are shown in Fig. 4 for a waveguide wall thickness of 1.27 mm. A fair agreement between the theoretical and experimental results justifies the validity of the analysis. The data presented converge for $N = 5$. All computations have been carried out for $N = 5$. It is found that the numerical value changes only at the second decimal points when N is increased from 3 to 5. It is also been found that for $N = 5$, the results converges $m = 20$, $n = 20$. In the computations, $m = 30$ and $n = 30$ have been taken for getting sufficient and accurate data.

Acknowledgment

The authors thank the Director, Space Applications Centre (ISRO), Ahmedabad, India, and Indian National Science Academy, All India Council for Technical Education, New Delhi, India, for support.

References

[1] C. D. Montgomery, R. H. Dickie, and E. M. Purcell, *Principles of Microwave Circuits* (MIT Radiation Laboratory Series, vol. 8). New York: McGraw-Hill, 1948.
[2] I. Lebedev, *Microwave Engineering.* Moscow, Russia: MIR Publishers, 1974.
[3] J. L. Altman, *Microwave Circuits.* New York: Van Nostrand, 1964.
[4] W. H. Watson, *The Physical Principles of Waveguide Transmission and Antenna System.* London, U.K.: Oxford Univ. Press, 1947.
[5] N. Marcuvitz, *Waveguide Handbook.* New York: Dover, 1965.
[6] B. N. Das and P. V. D. S. Rao, "Analysis of a junction between rectangular and circular guides with collinear axes," *Proc. Inst. Elect. Eng.*, vol. 138, pt. H, no. 4, pp. 265–268, Aug. 1991.
[7] ——, "Analysis of transition between rectangular and circular waveguides," *IEEE Trans. Microwave Theory Tech.*, vol. 39, pp. 357–359, Feb. 1991.
[8] B. N. Das, A. Chakrabarty, and N. V. S. N. Sharma, "S-matrix of a slot-coupled T-junction between rectangular waveguides," *IEEE Trans. Microwave Theory Tech.*, vol. 38, pp. 779–781, June 1991.
[9] B. N. Das, P. V. D. S. Rao, and A. Chakrabarty, "Narrow wall axial slot-coupled T-junction between rectangular and circular waveguides," *IEEE Trans. Microwave Theory Tech.*, vol. 37, pp. 1590–1596, Oct. 1989.
[10] B. N. Das and P. V. D. S. Rao, "Analysis of cascaded sections of T-junctions between rectangular waveguides," *IEEE Trans. Microwave Theory Tech.*, vol. 39, pp. 92–97, Jan. 1991.
[11] L. G. Joseffson, "Analysis of longitudinal slots in rectangular waveguides," *IEEE Trans. Antennas Propagat.*, vol. AP-35, pp. 1351–1357, Dec. 1987.
[12] R. F. Harrington, *Time-Harmonic Electromagnetic Fields.* New York: McGraw-Hill, 1961.
[13] G. Markov, *Antennas.* Moscow, U.S.S.R.: Progress Publishers, 1965.